

# Evaluation of Fault Rupture Hazard Mitigation

Tom Shantz<sup>1</sup>, Fadel Alameddine<sup>2</sup>, Jaro Simek<sup>2</sup>, Mark Yashinsky<sup>2</sup>, Martha Merriam<sup>3</sup>, and Mike Keever<sup>4</sup>

Caltrans recently performed an in-house study to develop rationale for establishing probabilistic design criteria with regard to fault rupture hazard. The study consisted of the development of several alternative bridge designs with varying capacity for displacement offset. A fragility curve and cost estimate was developed for each alternative design. Using the fragility curves and a simple probabilistic fault-offset model, the probability of collapse was calculated for each alternative design. The mitigation efficiency, defined as the decrease in collapse probability (based on a 75-year design life) divided by the increase in bridge cost, was compared to typical mitigation efficiencies associated with implementing Caltrans seismic design criteria for shaking hazard. The study found that while designing a bridge to accommodate large fault offset may double costs, the corresponding reduction in collapse probability is substantial, leading to mitigation efficiencies twice as large as those obtained in typical design practice for shaking hazard.

---

<sup>1</sup> Research Engineer, Caltrans, 5900 Folsom Blvd Sacramento, CA 95819

<sup>2</sup> Bridge Engineer, Caltrans, 1801 30<sup>th</sup> Street, Sacramento, CA 95816

<sup>3</sup> Engineering Geologist, Caltrans, 5900 Folsom Blvd Sacramento, CA 95819

<sup>4</sup> Supervising Bridge Engineer, Caltrans, 1801 30<sup>th</sup> Street, Sacramento, CA 95816

## INTRODUCTION

Many bridges in California span earthquake faults. The number of active faults in California is large and avoidance is often impractical. Furthermore, many bridges were constructed well before the presence of an underlying fault was recognized. If a fault ruptures beneath a bridge, the bridge is subjected to both quasi-static displacement offset and strong ground shaking. Simplified procedures for combining these demands have been developed through Caltrans funded research by Goel and Chopra (2008; 2009a; 2009b). Fault offsets typically range from 0.5 to 2 feet from a **M**6.5 strike slip earthquake to several tens of feet from a **M**8. Such potentially large demands present a formidable challenge to the engineer trying to satisfy a “no collapse” performance goal.

In the case of strike slip faults, the displacement offset is predominantly in the horizontal plane though small vertical offsets should be expected as well. Relatively small offset demands, typically up to about 2 feet, can be accommodated through column flexure. To accommodate larger displacement demands, strategies involving the use of large displacement capacity bearings, sliding, and catcher bents have been proposed. Some of these concepts have been applied on actual projects but experience with these techniques is limited and design strategies are still evolving.

In the case of reverse or normal faulting, depending upon the dip angle of the fault plane, displacement demands include both horizontal and vertical components. Since a bridge’s primary function is to resist gravity load, their ability to accommodate vertical offset is generally considered to be sufficient for moderate demands. There are limits, however, as several bridges collapsed under large vertical fault offsets during the 1999 Chi-Chi (MCEER, 2000) and 2008 Wen Chuan (EERI, 2008) earthquakes. Design strategies for vertical offset are less developed than for horizontal offset. The study reported here considers only horizontal offset though the authors believe the findings are generally applicable to the case of vertical offset as well.

In assessing a bridge’s vulnerability to potential fault offset, an assumption of worst-case scenario demand would tend to push the limits of both engineering capability and project budgets. Typically, probabilistic methods are used to assess the potential hazard. For shaking hazard, Caltrans uses a 5% in 50-year probability of exceedence (975-year return period) as part of the specification of the design response spectrum. This same hazard level is currently being used to define potential offset demand for fault crossings.

Recently, two contradictory viewpoints have questioned the use of the 975-year hazard level, one arguing for a lower *design hazard level* (DHL), the other advocating a higher DHL. The fundamental argument for each position can be summarized as follows:

### *Case for a lower design hazard level*

The cost of mitigating fault rupture hazard is significantly higher than that of mitigating shaking hazard. Thus, to avoid inefficient spending, the design hazard for fault rupture should be reduced to something less than that of shaking hazard.

#### *Case for an increased design hazard level*

The consequences of fault rupture are more severe than that of ground shaking. This higher potential for collapse warrants consideration of design events that are less probable than that of the shaking hazard.

On the surface, both arguments are compelling despite their contradictory positions. In order to shed light on this issue Caltrans initiated an in-house study to evaluate the merit of these arguments. This paper presents the results of that study.

## **METHODOLOGY**

To evaluate the benefits and costs associated with increased or reduced design hazard levels for fault rupture, these benefits and costs were compared to those obtained by current design practice for ground shaking hazard. The benefits and costs were calculated in terms of “mitigation efficiency”, defined in (1).

$$\text{mitigation efficiency} = \frac{\text{reduction in 75 year collapse probability}}{\text{cost of mitigation (\$/SF)}} \quad (1)$$

Mitigation efficiency was compared for the case of a hypothetical bridge spanning the Hayward Fault, a large active fault in the San Francisco Bay area. In order to estimate mitigation efficiency, three relationships are required:

1. *Hazard curves* are needed to describe the rate at which the demand parameter exceeds a particular value. In this study two demand parameters are considered: peak ground acceleration (PGA) and fault offset.
2. *Fragility curves* are needed to describe the probability that the bridge will collapse as a function of the demand parameter.
3. *Cost curves* are needed to describe the cost impact of designing a bridge to different levels of performance.

In order to compare mitigation efficiency for several levels of design, a baseline bridge configuration was considered along with three variants, two of which included use of large displacement capacity isolation bearings. Details of these bridges are presented in the next section, followed by a description of the development of the hazard and fragility curves.

### **Study Bridge**

The baseline bridge was a five span, concrete box girder, 690 feet in length. A typical section is shown in Figure 1a. Two column heights were considered in the study, 22-foot tall and 50-foot tall, but only the results for the 22-foot tall column are presented here. In addition to the baseline bridge, three additional variants were designed to the point that they could be reasonably cost-estimated. These three variants were designed to provide increasing levels of displacement capacity. The first variant utilized large single shaft foundations and larger diameter columns to increase displacement capacity. The second variant used a single shaft foundation as well, but also included four friction pendulum bearings at each bent and at the

abutments. A typical section for this variant is provided in Figure 1b. The use of isolation bearings allowed the second variant to use smaller diameter columns than that of the first variant. Finally, the third variant is similar to the second except that it uses larger displacement capacity friction pendulum bearings than the second variant as well as larger diameter columns. Table I provides an overview of the different bridge configurations.

TABLE I: SUMMARY OF DESIGN VARIANTS

Bridge Design	Foundation type	Column Diameter (ft)	Bearing Diameter (ft)	1st mode period (s)
Baseline	Pile group	6	-	0.85
Variant 1	Shaft	8.25	-	0.85
Variant 2	Shaft	6	6	4.5
Variant 3	Shaft	7	8	4.5

### Hazard and Fragility Curves for Shaking (only) Demand

A hazard curve for a location directly on the Hayward Fault was developed using the USGS Deaggregation website (USGS, 2008) and is shown in Figure 2a. The hazard curve selected for this study uses PGA as the demand parameter and assumes an upper 30-meter time averaged shear wave velocity ( $V_{S30}$ ) of 300 m/s.

Figure 3 presents a table of approximate target values and corresponding fragility curves for optimistic and pessimistic views of expected column performance. These target values were selected based on the collective judgment of the study team. The curves rely

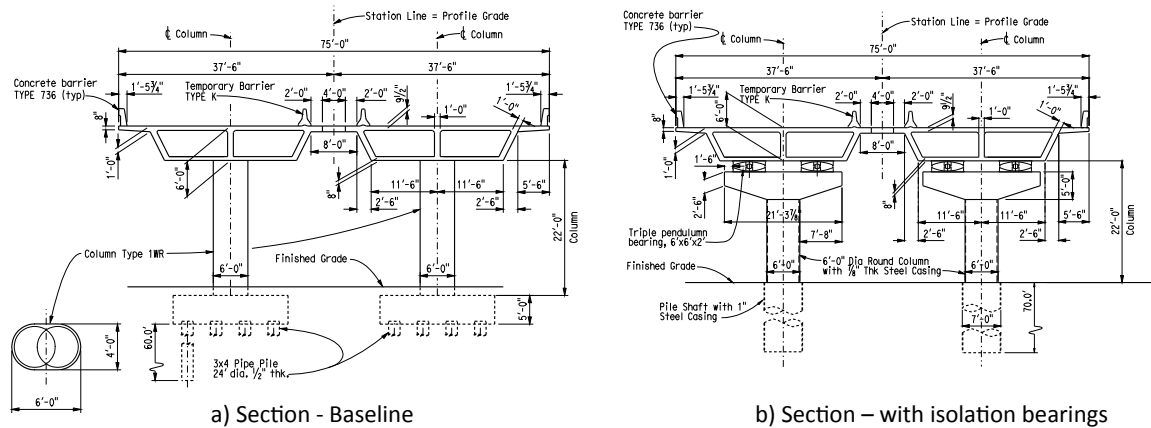


Figure 1: (a) cross-section for Baseline bridge. (b) cross-section for Variant 2.

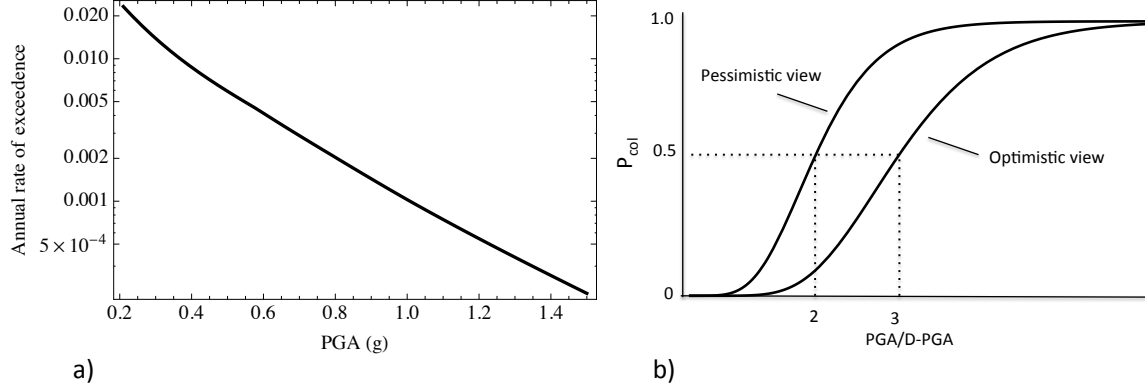


Figure 2: (a) Hazard curve for site on the Hayward Fault with  $V_{S30}$  of 300 m/s; (b) fragility curves based on the ratio of PGA and *design* PGA as the demand parameter.  $P_{col}$  refers to the probability of collapse.

on displacement ductility,  $\mu_{\Delta}$ , defined in (2), as the demand parameter.

$$\mu_{\Delta} = \frac{\Delta_D}{\Delta_y} \quad (2)$$

In (2)  $\Delta_D$  represents displacement demand and  $\Delta_y$  represents yield displacement. The approximate target values can be fit reasonably well by modeling the fragility curve as a cumulative distribution function (CDF) of a lognormal distribution with standard deviation  $\sigma_{LN}=0.3$  and median equal to the  $\mu_{\Delta}$  corresponding to a 50% probability of collapse. If it is assumed that a particular *design*-PGA (D-PGA) corresponds to a ductility demand of 4, consistent with Caltrans Seismic Design Criteria (SDC, 2010), the fragility curves in Figure 3 can be recast in terms of PGA as shown in Figure 2b.

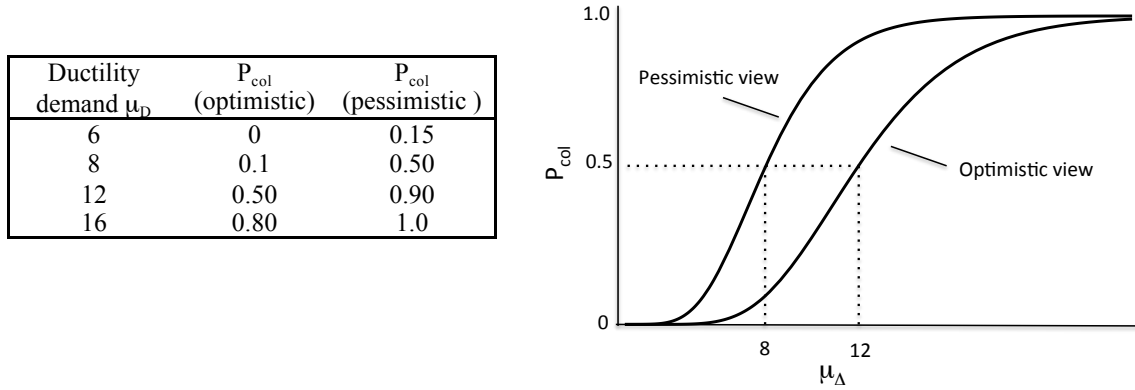


Figure 3: Column performance estimates reflecting a range of expert opinion.  $P_{col}$  refers to the probability of collapse. The corresponding fragility curves were modeled as lognormal CDF's with  $\sigma_{LN}=0.30$ .

## Hazard and Fragility Curves for Shaking and Fault Offset Demand

For the case of combined ground-shaking and fault offset demand, dynamic and quasi-static displacement demands act together. These demands are characterized separately here and later combined in the calculation of collapse probability.

The fault-offset demand is described by the hazard curve shown in Figure 4a. This curve was developed using simplified procedures described in Abrahamson (2008), with an expanded explanation provided in Shantz (2013). This approach assumes that the fault ruptures predominantly in a narrow range of magnitudes, centered on a characteristic magnitude,  $M_c$ . In this study  $M_c$  was estimated to be **M7**. It is important to note that while the hazard curve in Figure 4a represents the rate of exceedence for different levels of fault offset, this offset demand is shared between bridge components on *both* sides of the fault. Thus, a 2-foot fault offset demand corresponds to a 1-foot demand on either side of the fault. This factor of 2 difference between fault offset and bridge demand will be accounted for when the hazard and fragility curves are used to calculate the collapse probability, described in the next section.

Figure 4b presents the distribution of peak displacement demands due to ground-shaking resulting from a characteristic earthquake for the cases of not using isolation bearings (Baseline and Variant 1 designs) and including isolation bearings (Variants 2 and 3). Each curve is characterized by a lognormal distribution with median equal to the spectral displacement at the first mode periods given in Table I. An average of the Campbell and Bozorgnia (2008) and Chiou and Youngs (2008) ground motion prediction equations was used to calculate the median and standard deviation of the distribution for each of the two cases.

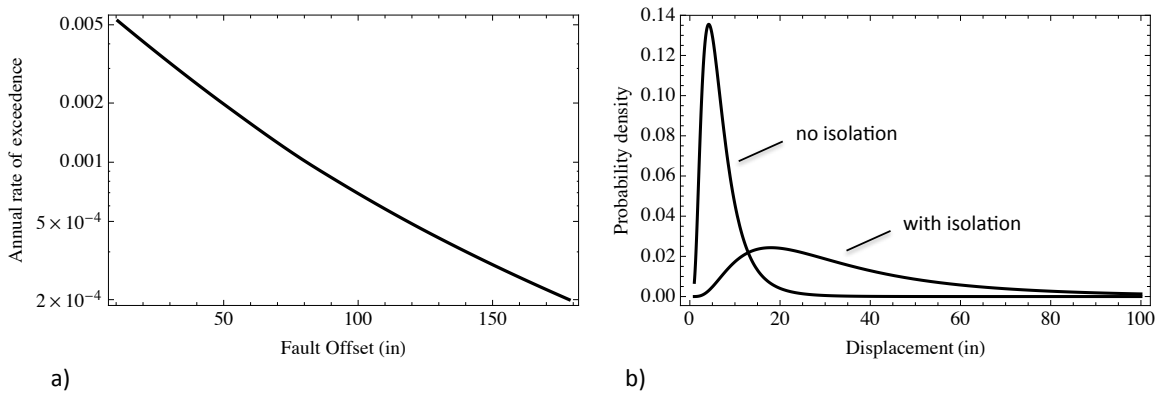
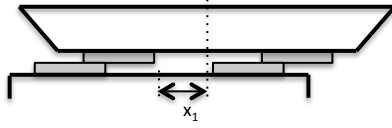


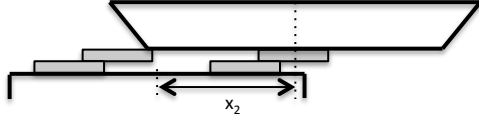
Figure 4: (a) Hazard curve for fault-offset along the Hayward fault; (b) Distribution of peak displacement demand due to ground shaking. Two cases are shown: without isolation,  $T_1=0.85s$  and  $\sigma_{LN}=0.59$ ; with isolation,  $T_1=4.5s$  and  $\sigma_{LN}=0.71$ .

The fragility curves in Figure 3 can be used for the Baseline and Variant 1 design cases since they don't utilize isolation bearings. For the Variant 2 and 3 design cases, fragility curves were developed as shown in Figure 5. It should be emphasized that the development of these curves was highly judgmental and assumed the superstructure will slide over the isolation bearings once the bearing displacement capacity is reached. Design details to ensure such sliding have not yet been physically tested.

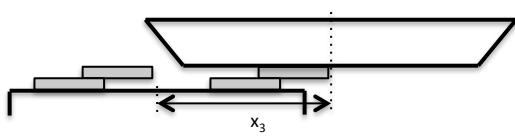
Case 1:  $x_1$  = full isolator displacement capacity



Case 2: center of mass of superstructure is located directly above the center of the fully extended isolator



Case 3: center of mass of superstructure is located just outside the fully extended isolator's edge



Disp (in)	6'x6' bearing	8'x8' bearing	$P_{col}$ (optimistic)	$P_{col}$ (pessimistic)
$X_1$	51	68	0	0
$X_2$	125	140	0.20	0.50
$X_3$	161	188	0.50	0.80

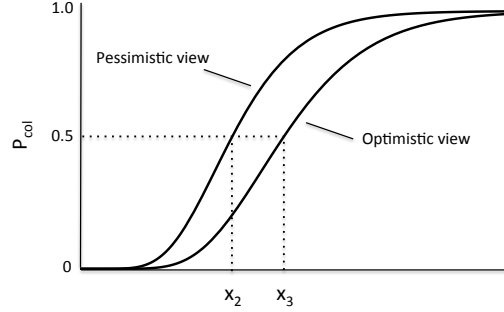


Figure 5: Development of fragility curves for a bridge with isolation bearings. The fragility curves are described by a lognormal normal distribution and assume a standard deviation  $\sigma_{LN} = 0.30$ .

## Calculating Collapse Probability

In order to calculate the reduction in 75-year collapse probability, the numerator in (1), the annual probability of collapse,  $P_{col-1}$ , for different design levels must first be calculated. This annual probability is then converted to a 75-year probability. The calculation for shaking (only) demand will be presented first and then extended to the case for combined shaking and fault offset.

### *Shaking (only) case*

The contribution to the annual probability of collapse,  $P_{col-1}$ , from a narrow range of demand, centered on  $z_i$  and with small width  $\Delta z$ , is given in (3):

$$\Delta P_{col-1} = P[z_i] \cdot F(z_i) \quad (3)$$

In (3)  $P[z_i]$  = the annual probability of demand  $z$  falling within the range  $z_i - \Delta z/2$  and  $z_i + \Delta z/2$ ;  $F(z_i)$  is a fragility curve, generally represented as a cumulative distribution function. For the case of shaking demand, the fragility curve is given in Figure 2b and the demand parameter  $z$  corresponds to PGA. Let  $\lambda(z)$  define a hazard curve, such as that given in Figure 2a.  $\lambda(z_i - \Delta z/2) - \lambda(z_i + \Delta z/2)$  = the annual *rate* that demand parameter  $z$  will fall in the interval centered on  $z_i$  and  $\Delta z$  wide. When this rate is small it is approximately equal to the probability of  $z$  falling in the same interval. (e.g. the difference between a 1/50 rate and 1/50 probability is less than 1%). Since typical rates of interest considered here meet this *small* criterion  $P[z_i]$  can be approximated as

$$P[z_i] \cong \lambda(z_i - \Delta z/2) - \lambda(z_i + \Delta z/2) \quad (4)$$

Finally, we can utilize the Total Probability Theorem and calculate the total annual probability of collapse by summing across the contributions from all possible demands as given in (5).

$$P_{col-1} = \sum_{z_i} \Delta P_{col-1} \quad (5)$$

The annual probability of collapse can be extended to a 75-year time interval using (6).

$$P_{col-75} = 1 - (1 - P_{col-1})^{75} \quad (6)$$

### ***Shaking and Fault-Offset case***

For the case of combined quasi-static and dynamic demand, the same approach as presented in the previous section can be applied, but with minor modification. If dynamic demand is ignored, equations (3) through (6) can be applied to the quasi-static demand case where demand parameter  $z$  corresponds to *half* the fault-offset displacement,  $\lambda(z)$  corresponds to the hazard curve given in Figure 4a, and the fragility curve  $F(z)$  corresponds to that shown in Figures 3 or 5 depending on use of an isolation bearing. When dynamic demand is included these same equations apply except that in (3) a modified fragility, defined in (7), must be used instead of  $F(z_i)$ .

$$\bar{F}(x_i) = \int F\left(\frac{x_i}{2} + y\right) \cdot g(y) dy \quad (7)$$

In (7)  $x_i$  is the fault offset,  $y$  is the peak dynamic displacement, and  $g(y)$  is the probability density function describing the distribution of  $y$ .  $g(y)$  is given in Figure 4b for cases with and without use of isolation bearings. Conceptually, (7) describes the fragility for a given fault offset, averaged over a range of possible peak dynamic displacement contributions that are weighted by their probability.

### **Calculation of Mitigation Efficiency**

Using the methods described above, a 75-year collapse probability was calculated for both optimistic and pessimistic assumptions of fragility for each design option. These results are summarized and plotted in Figure 6. Costs for each design option were based on detailed cost breakdowns for each design option, with the baseline bridge coming in just under \$8M and the Variant 3 design coming in just over \$21M. The results demonstrated that while Variant 1 led to a modest reduction in collapse probability relative to the Baseline option, the collapse probability remained high. In order to achieve substantial reduction in collapse probability use of large isolation bearings was required. Use of such bearings resulted in an approximate doubling of cost, driven primarily by the added cost of the individual bearings and the need for a larger substructure to support them.



The mitigation efficiency, as defined in (1), is equal to the slope of the curve in Figure 6b. Since Variant 2 appears to be the most logical alternative to the Baseline design option, this design option was used to estimate the mitigation efficiency. As shown in Figure 6b, the mitigation efficiency for Variant 2 is approximately a 1% reduction in  $P_{\text{col-75}}$  per \$10 psf increase in cost.

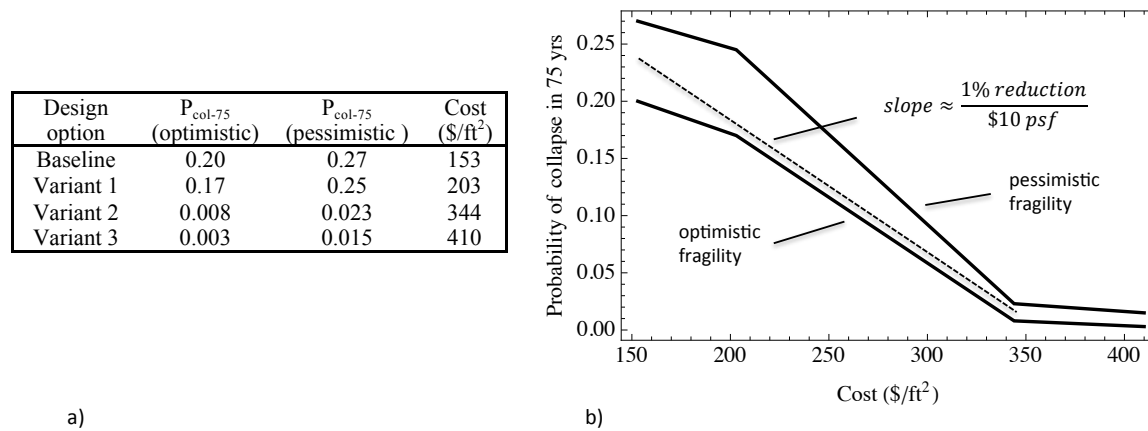


Figure 6: (a) Summary table of collapse probabilities and costs for each design considered; (b) plot of Fig. 6a data and approximate slope fit (mitigation efficiency)

For the shaking (only) case, since the fragility curve (see Figure 2b) was defined in terms of *design*-PGA, each D-PGA level represented a different design option. The impact of D-PGA on collapse probability is shown in Figure 7a. Generally, the collapse probabilities due to shaking (only) were substantially lower than that due to fault offset and shaking together. Since Caltrans design criteria includes consideration of a 5% in 50-year (975-year return period) ground motion, the D-PGA for the study scenario would have been 1 g. At this design level the 75-year collapse probability was estimated to be between 0.02% and 0.4%.

In order to account for the cost impact of designing to different PGA levels, results from a study by Ketchum (2004) were used to create the cost curve shown in Figure 7a (inset). The two plots in Figure 7a were then used to generate Figure 7b, which describes the 75-year collapse probability as a function of cost, similar to Figure 6b. To estimate mitigation efficiency, a representative slope for these curves was approximated using the right-most region of the curves since this region corresponds to Caltrans' current design practice. The mitigation efficiency for shaking hazard was estimated to be about 0.5% reduction in  $P_{\text{col-75}}$  per \$10 psf increase in cost, about half that for the case of fault-offset hazard.

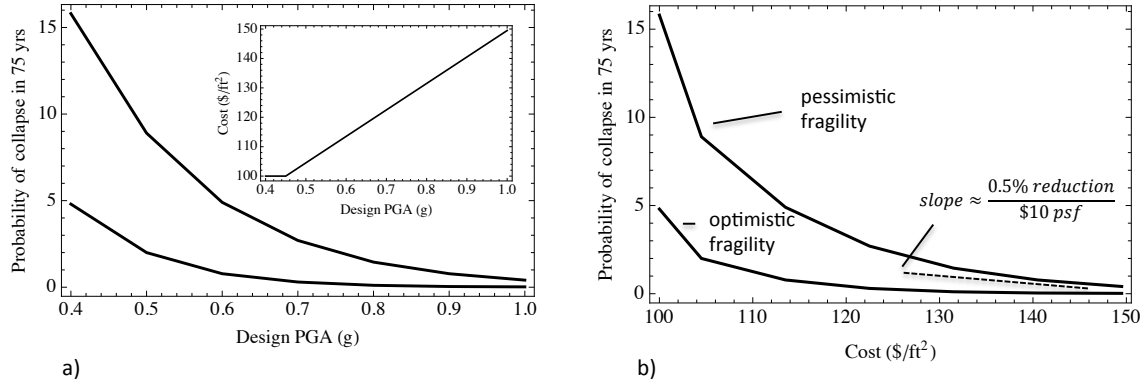


Figure 7: (a) 75-year collapse probability due to shaking as a function of *Design-PGA*. (a)-inset: bridge cost as a function of *Design-PGA* (based on Ketchum, 2004); (b) 75-year collapse probability as a function of cost and approximate slope fit (mitigation efficiency).

## CONCLUSION

For the Hayward Fault scenario, it was found that mitigation for fault-offset hazard using isolation bearings is roughly twice as cost efficient in reducing collapse probability as that achieved by normal seismic design practice for shaking hazard. The rough doubling of cost associated with use of isolation bearings was overshadowed by their effectiveness in reducing 75-year collapse probability from an unacceptably large range of 20 to 27% to only 1 to 2%.

How does this result reflect on the merits of increasing or decreasing the design hazard level? The argument for lowering the DHL is clearly flawed because it focuses solely on cost and fails to consider the much heightened collapse risk at fault crossing locations as well as the effectiveness of potential mitigation measures at reducing that risk. The argument for increasing DHL is generally correct in that it recognizes the substantially heightened collapse risk at fault crossings relative to shaking (only) hazard.

If the decision to mitigate fault-offset hazard is recast in terms of achieving a target return (reduced collapse probability) for a unit investment in mitigation, then it is unlikely that a single DHL can be found that, when applied to all design scenarios, will result in mitigation decisions that correspond to the target return on investment. The “correct” DHL will be depend on the particular fault’s characteristic magnitude and slip rate, as well as details of the particular bridge. As an alternative to the single DHL concept, a streamlined calculation of mitigation efficiency could be performed utilizing semi-standardized isolation bearing design that would allow for standardized fragility and cost curves. Under this framework, mitigation efficiency could be readily calculated as part of the fault-offset hazard calculation and then used to determine the merit of employing mitigation measures.

Finally, a brief discussion is warranted on the general applicability of the Hayward Fault scenario used in this study. Two factors, characteristic magnitude and slip rate, most affect applicability to other locations. An increase in slip rate will result in an increase in mitigation efficiency. Slip rates of active California faults range from near zero to 35 mm/yr on several segments of the San Andreas Fault (Dawson and Weldon, 2012). A slip rate of 9 mm/yr was

used for the Hayward Fault scenario in this study. The impact of magnitude is somewhat counter-intuitive since larger magnitudes, though more damaging when they occur, are far less likely to occur for a given slip rate. Thus, once the characteristic magnitude is large enough to produce fault offsets that exceed bridge columns flexural capacity, the potential for collapse quickly increases. The impact of characteristic magnitude on mitigation efficiency is likely to peak roughly around **M6.7** and decrease for larger magnitudes. In this study a **M7** scenario was used.

## REFERENCES

Abrahamson, N., 2008, Appendix C, Probabilistic Fault Rupture Hazard Analysis, San Francisco PUC, General Seismic Requirements for the Design on New Facilities and Upgrade of Existing Facilities

Campbell, K., and Bozorgnia, Y., 2008, NGA ground motion model for the geometric mean horizontal component of PGA, PGV, PGD, and 5% damped linear elastic response spectra for periods ranging from 0.01 to 10 s.: *Earthquake Spectra*, Vol.24, pp.139-172.

Chiou, B., and Youngs, R., 2008, An NGA model for the average horizontal component of peak ground motion and response spectra: *Earthquake Spectra*, Vol.24, pp.173-216.

Dawson, T., and Weldon, R., 2012, UCERF 3 Appendix B: Geologic slip-rate data and geologic deformation model (Draft version dated July 9, 2012):  
[http://wgcep.org/sites/wgcep.org/files/AppendixB\\_GeologicDeformationModel\\_20120709.pdf](http://wgcep.org/sites/wgcep.org/files/AppendixB_GeologicDeformationModel_20120709.pdf)

Earthquake Engineering Research Institute (EERI), 2008, Special Earthquake Report, “The Wenchuan, Sichuan Province, China, Earthquake of May 12, 2008”, October 2008.

Goel, R.K. and Chopra, A.K. 2008. “Analysis of Ordinary Bridges Crossing Fault-Rupture Zones,” Report No. UCB/EERC-2008/01, Earthquake Engineering Research Center, University of California, Berkeley, CA.

Goel, R.K. and Chopra, A.K. 2009a. “Linear Analysis of Ordinary Bridges Crossing Fault-Rupture Zones.” *Journal of Bridge Engineering*, 14(3): 203-215.

Goel, R.K. and Chopra, A.K. 2009b. “Nonlinear Analysis of Ordinary Bridges Crossing Fault-Rupture Zones.” *Journal of Bridge Engineering*, 14(3): 216-224.

Ketchum, M., Chang, V., and Shantz, T. , 2004. *Influence of Design Ground Motion Level on Highway Bridge Costs*. Report No. Lifelines 6D01, University of California, Pacific Earthquake Engineering Research Center, Berkeley, CA

Seismic Design Criteria (SDC 1.6), 2010, Caltrans Office of Earthquake Engineering,  
[http://www.dot.ca.gov/hq/esc/earthquake\\_engineering/SDC\\_site/](http://www.dot.ca.gov/hq/esc/earthquake_engineering/SDC_site/)

Shantz, T., 2013, “Caltrans Procedures for Calculation of Fault Rupture Hazard”,  
[http://www.dot.ca.gov/newtech/structures/peer\\_lifeline\\_program/docs/Caltrans\\_Procedures\\_for\\_Fault\\_Rupture\\_Hazard\\_Calculation.pdf](http://www.dot.ca.gov/newtech/structures/peer_lifeline_program/docs/Caltrans_Procedures_for_Fault_Rupture_Hazard_Calculation.pdf)

The Chi-Chi, Taiwan Earthquake of September 21, 1999: Reconnaissance Report  
Edited by G.C.Lee, C.H.Loh; MCEER-00-0003; 4/30/2000

USGS, 2008 Interactive Deaggregations (Beta), <https://geohazards.usgs.gov/deaggint/2008/>